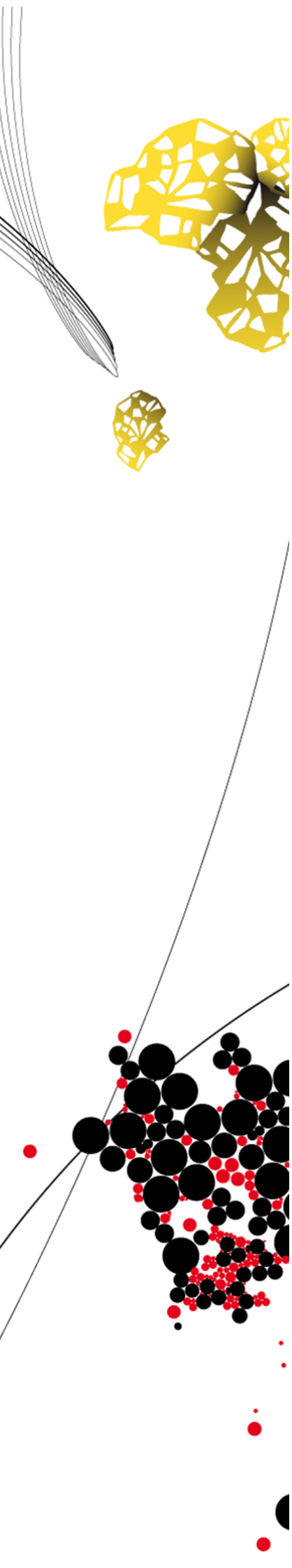

UNIVERSITY OF TWENTE.

Faculty of Electrical Engineering, Mathematics & Computer Science

Investigation of TOA/TDOA Localization in the Presence of Receiver Sensor Position Error

Tatsuki Fujioka

B.Sc. Thesis
June 2022

Supervisors University of Twente:
Dr. Ir. Andre Kokkeler
Dr. Ing. Anastasia Lavrenko
Dr. Ing. Nikolaos Alachiotis

Radio Systems Group
Faculty of Electrical Engineering,
Mathematics and Computer Science
University of Twente
P.O. Box 217
7500 AE Enschede
The Netherlands

Summary

In light of growing use of self-navigation robots and potential application of unmanned arial vehicles (UAVs), the accurate radio localization is becoming ever more and more crucial. Among other things, localization accuracy is sensitive to the accurate knowledge of receiver sensor positions. This paper studies performance of time-of-arrival (TOA) and time-difference-of-arrival (TDOA) localization with square and triangular sensor deployments in the presence of random errors in sensor positions due to the mobility of sensor nodes. It begins with the derivations of Cramer-Rao lower bound (CRLB) and three closed-form estimation methods namely linear least squares (LLS), weighted linear least squares (WLLS) and 2-step weighted linear least squares (2WLLS). Then, simulations of the TOA- and TDOA-based localization using the 2WLLS with both deployments are conducted and the comparisons of the root-mean-square position errors (RMSEs) are made. The comparison shows that the highest accuracy is achieved by the TOA-based localization with the square deployment, followed by the TDOA-based localization with the square deployment. The accuracy of the latter however, differs by only 0.31dB for the low sensor position error.

Contents

Chapter 1

Introduction

1.1 Radio Localization

In signal processing, one of the well-studied subjects is location estimation. As technology of unmanned aerial vehicles (UAVs) has advanced rapidly in the recent years, radio localization using UAVs has become one of the potential applications for the future. Although location determination techniques such the ones using radar and GPS have long been studied, the application of the radio localization using UAVs as anchor nodes for radio localization is relatively new in the signal processing field. The main advantage of the use of mobile sensor nodes is that it could make a deployment of sensor nodes over wide coverage of area easier and quicker thanks to their mobility. Sensor node mobility however, introduces an additional source of error to the localization process. This work investigates its effects on the location estimation performance.

For the localization of a target at an unknown location, the common measurement methods are Time of Arrival (TOA), Time Difference of Arrival (TDOA), Angle of Arrival (AOA) and Received Signal Strength (RSS) [1]. In mobile outdoor scenarios however, the localization with AOA or RSS is not suitable since the former may require weighty and complex antenna array equipment and the latter has relatively low accuracy compared to the other measurement methods. Therefore, in this work the TOA and the TDOA are studied.

Target localization using the TOA or the TDOA is a complicated problem since both measurement methods result in a system of nonlinear equations that relate the measurements to the target location. To solve the problem, there are two types of algorithms: iterative algorithms including first-order Taylor series method and the Newton-Raphson method [2], and the closed-form solution methods including linear least squares (LS), weighted linear least squares (WLS), two-step weighted linear least squares (2WLS) and subspace methods [2]. The iterative methods generally have high accuracy but require high computational complexity due to the iterative processes and the need to first ac-

quire a 'good' initial solution to ensure the convergence of the final solution. In contrast, the closed-form solution methods have low computational complexity, which is preferable for target localization using UAVs since computational resources are often limited. The accuracy of the closed-form solution methods varies depending on whether statistical knowledge of the measurement parameters is known or not. Thus, the LS and subspace methods do not require the statistical knowledge but has they have lower accuracy whilst the WLS and 2WLS require statistical knowledge which generally results in a higher localization accuracy.

Irrespective of the location estimation method, the localization accuracy is influenced by the distance measurement error as well as the accuracy of the anchor position knowledge. When one places receivers on UAVs, the mobility of the UAVs causes uncertainty of the receiver positions, which degrades the accuracy of the location estimations. Several works have considered the effect of sensor node mobility on localization accuracy. In [3] and [4], 2WLLS-based methods have been proposed that account for the sensor node mobility but no direct comparisons between the two localization methods were given. While this has been a topic of increasing interest recently, there are still some fundamental gaps in understanding how sensor node position uncertainty affects location estimation performance. Particularly, when compared between TOA and TDOA leads to research questions in the following section.

1.2 Research Questions

This work considers the effect of anchor node position uncertainty on location estimation performance of TOA- and TDOA-based localization using closed-form solution methods in the presence of distance measurement errors. More specifically, the research questions it addresses are

- What is the localization accuracy of TOA- and TDOA-based localization in the presence of the anchor node position error and the distance measurement error?
- What is the effect of a geometrical configuration of sensor nodes on location estimation performance?
- Which one of the localization techniques is more suitable in presence of sensor position uncertainty?

1.3 Outline

The paper is organized as follows. In Chapter 2, basic principles of TOA- and TDOA-based localizations as well as models of measurement and sensor position errors are

described. Subsequently, formulations of LLS, WLLS and 2WLLS are presented in Chapter 3. In Chapter 4, simulation results of the 2WLLS method established in Chapter 3 are presented, which include TOA- and TDOA-based localizations with two different sensor deployments. Finally, based on the simulation results, conclusions are drawn in Chapter 5, in which the answers to the research questions are given.

Chapter 2

TOA/TDOA Localization Principles

2.1 TOA-based Localization

In this section, a basic principle of TOA-based localization as well as its geometrical interpretation are presented first in 2.1.1. Then, measurement and sensor position error models are introduced.

2.1.1 Basic Principle

TOA-based localization is a localization method that estimates an unknown target location based on a propagation time of a radio signal emitted from the target. A noise-free TOA-based localization model is illustrated in Figure 2.1, where the sensor nodes located at $\mathbf{s}_i^o = [x_i^o \ y_i^o]$ are used to measure the radio signal emitted by the target source located at $\mathbf{u}^o = [x^o \ y^o]$. Assuming that the radio signal is emitted at time t_M and the propagation time, also known as time of flight between the target and the ith receiver, is τ_i, the TOA measurement at the ith sensor is given by [2]

$$t_i = \tau_i + t_M = \frac{\sqrt{(x_i^o - x^o)^2 + (y_i^o - y^o)^2}}{c} + t_M \tag{2.1}$$

where c is the propagation speed of the signal. Subtracting t_M from E.q.2.1 and multiplying it by the propagation speed c yields the distance between the target and the ith sensor as

$$r_i^o = ||\mathbf{u}^o - \mathbf{s}_i^o|| = \sqrt{(x_i^o - x^o)^2 + (y_i^o - y^o)^2}. \tag{2.2}$$

Equation 2.2 is a circular equation in which a possible target location exist on a circle centered at the corresponding sensor node. As the measurement at each sensor node provides a circle with different center and radius determined by r_i, the target location can be found at the point where all circles intersect (see Figure 2.1). Since the emission time of the radio signal t_M needs to be known to obtain the circular equation, a clock synchronization between the sensor nodes and the target source is required. Furthermore, it can

be seen that if the number of sensor nodes is 2, there exist two intersections of the circles. This is due to the fact that two linearly independent equations are required to obtain an unique solution from an equation that contains two unknown parameters. Therefore, to obtain an unique solution for the target location in 2 dimensional plane, at least three sensor nodes are needed. In case of TOA-based localization in 3 dimensional space, at least four sensor nodes are required to obtain an unique solution of a target location. Although TOA-based localization in practical situations is implemented in 3 dimensional space, the basic principle of TOA-based localization in 2 dimensional plane is the same as in 3 dimensional space. Therefore, 2 dimensional plane is considered for all localization methods and simulations in this paper.

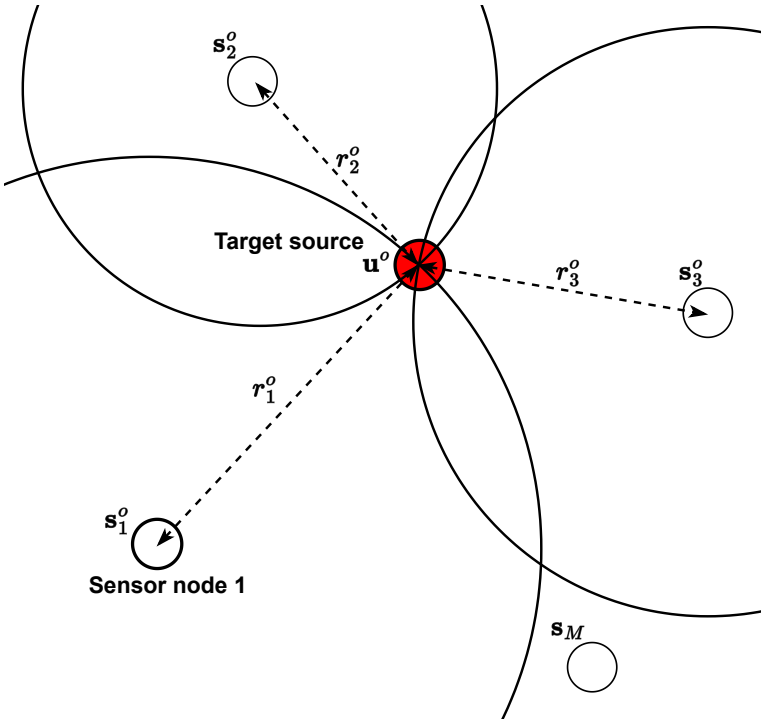

Figure 2.1: Noise-free TOA localization model

2.1.2 Measurement and Sensor Position Errors

In 2.1.1, a basic principle of a noise-free TOA-based localization model is described. In practice, the true TOA range measurement r_i^o is not available due to the measurement error. The range measurement with the zero-mean Gaussian measurement error n_i with standard deviation (STD) σ_i is [2]

$$r_i = \sqrt{(x_i^o - x^o)^2 + (y_i^o - y^o)^2} + n_i. \tag{2.3}$$

In an outdoor TOA-based localization with mobile sensors nodes such as UAVs, the mobile sensors cannot exactly be at desired positions due to the mobility of UAV and the

inaccuracy of the GPS unit equipped on the UAVs. Since an exact sensor node position is not available in practice, we have that

$$\mathbf{s}_i^o = \mathbf{s}_i - \mathbf{n}_{si}, \tag{2.4}$$

where $\mathbf{s}_i$ is the sensor position provided by the GPS unit and n_{si} is the sensor position error due to the mobility and the inaccuracy of the GPS unit, which is assumed to be zero-mean Gaussian with STD σ_{si}.

The TOA localization model in the presence of the distance measurement error and the sensor position error is illustrated in Figure 2.2. It must be noted that the measurement error and the sensor position error are added only to the first sensor node for simplicity of the illustration. As can be seen in Figure 2.2, there is no intersection where all three circles lie due to the introduced errors. To obtain an estimate of the target location which most likely lies on a point where all three circles are closest to each other, LLS , WLLS and 2WLLS can be used.

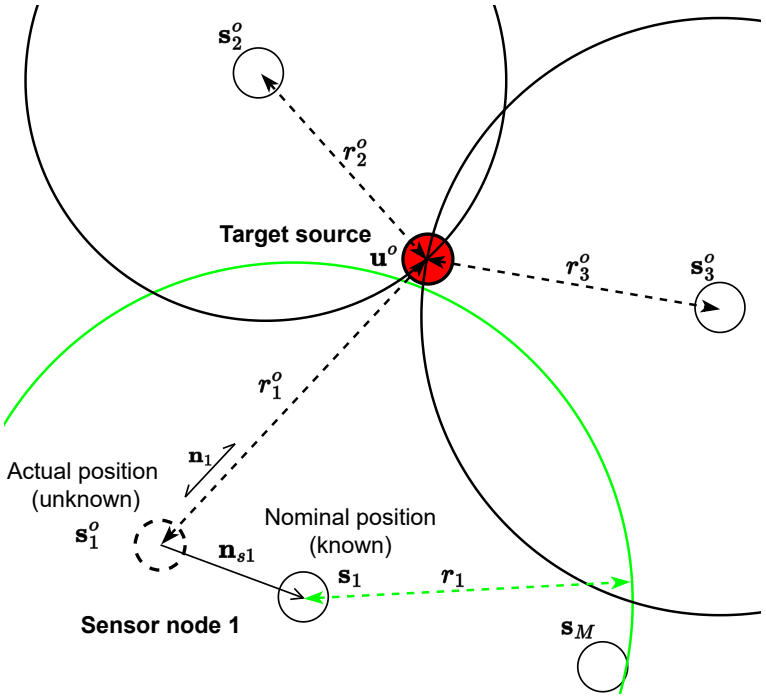

Figure 2.2: TOA localization model in presence of distance measurement error and sensor position error for first sensor node

2.2 TDOA-based Localization

Similarly, in this section, a basic principle of TDOA-based localization as well as its geometrical interpretation are presented first in 2.1.1. Then, measurement and sensor position error models are presented.

2.2.1 Basic Principle

In line with the TOA localization illustrated in Figure 2.1, the sensor and the target positions for the TDOA localization are defined as $\mathbf{s}_i^o = [x_i^o \; y_i^o]$ and $\mathbf{u}^o = [x^o \; y^o]$ respectively, where the subscript denotes the index of the sensor. Principally, a measurement at each sensor node of TDOA-based localization is expressed by the same equation as in Equation 2.2.However, in contrast to the TOA-based localization, the clocks of the sensors and the target source are not synchronized, leaving the emission time t_M unknown. For this reason, time difference between the measurements of the different sensors must be taken. Let the first sensor be a reference, subtracting the time measurement at the reference from the measurement at ith sensor yields the TDOA range measurement [5],

$$r_{i1}^o = \sqrt{(x_i^o - x^o)^2 + (y_i^o - y^o)^2} - \sqrt{(x_1^o - x^o)^2 + (y_1^o - y^o)^2}. \tag{2.5}$$

Equation 2.5 is a hyperbolic equation in which a possible target location lies on a hyperbola. The illustration of a noise-free TDOA-based localization model is shown in Figure 2.3. As the TDOA range measurement is obtained by taking the time difference between

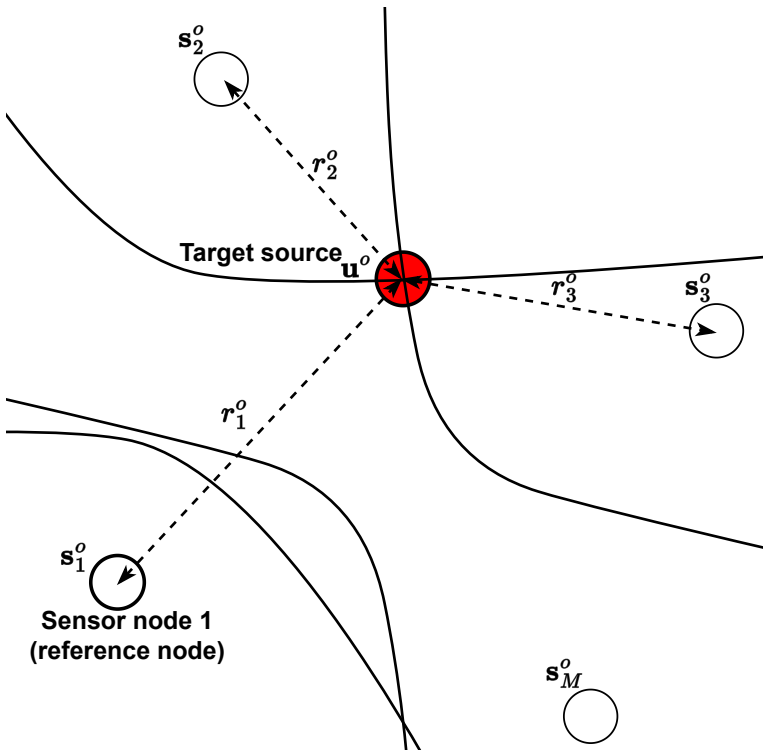

Figure 2.3: Noise-free TDOA localization model

the measurements at the reference sensor node and the other sensor nodes, the number of linearly independent TDOA range measurement equations is $M - 1$, where M is the total number of sensor nodes. This can be seen in Figure 2.3 where three sensor nodes including the reference sensor node are used. Since there exist two intersections

of the hyperbole, TDOA-based localization requires at least four sensor nodes to obtain an unique solution for the target location in 2 dimensional plane. Regarding the dimension of the given localization model, for the same reason stated as at the end of 2.1.1, 2 dimensional plane is considered.

2.2.2 Measurement and Sensor Position Errors

As shown in Equation 2.5, the TDOA range measurement is derived by taking the difference between the TOA measurements at the reference sensor and the other sensor nodes. Since the TOA measurement at each sensor contains the measurement noise as in Equation 2.3, the TDOA measurement in the presence of the distance measurement error r_{i1} contains a distance measurement noise $n_{i1} = n_i - n_1$, resulting in

$$r_{i1} = \sqrt{(x_i^o - x^o)^2 + (y_i^o - y^o)^2} - \sqrt{(x_1^o - x^o)^2 + (y_1^o - y^o)^2} + n_{i1} \tag{2.6}$$

or

$$r_{i1} + \sqrt{(x_1^o - x^o)^2 + (y_1^o - y^o)^2} = \sqrt{(x_i^o - x^o)^2 + (y_i^o - y^o)^2} + n_{i1}. \tag{2.7}$$

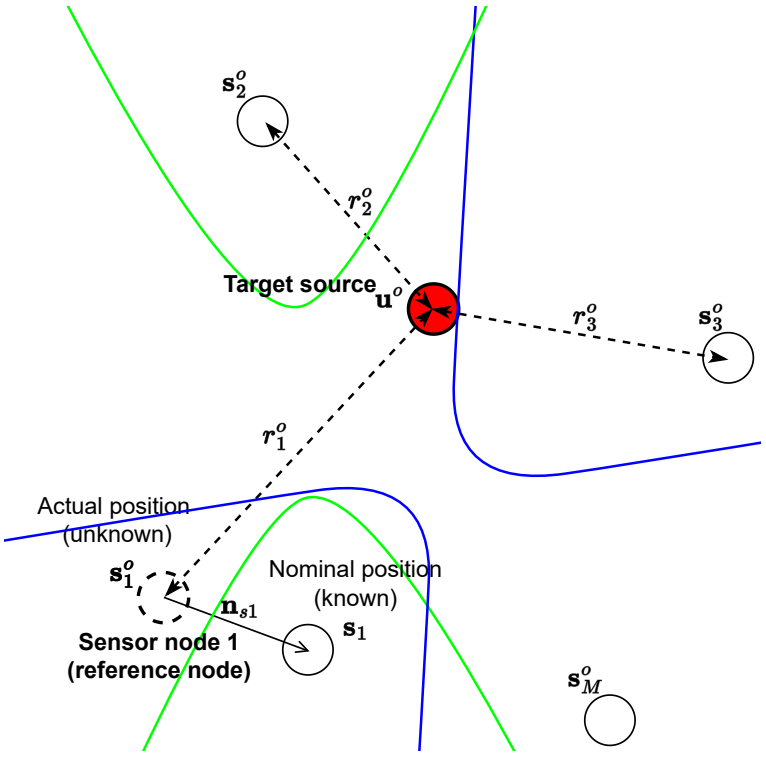

Figure 2.4: TDOA-based localization model in presence of distance measurement error and sensor position error

As for the sensor position error, again, the positions $\mathbf{s}_i^o = \mathbf{s}_i - \mathbf{n}_{si}$ are considered. Figure 2.4 illustrates the TDOA-based localization model in the presence of the two errors.

It must be noted that the two errors are added only to the reference node for simplicity of the illustration. Furthermore, it is worth noting that since the TDOA range measurements which forms the hyperbole are derived with respect to the TOA measurement at the reference sensor node, all TDOA range measurements and their hyperbole are affected by the two errors and thereby, potentially making the TDOA-based localization less accurate than the TOA-based localization.

Chapter 3

Closed-Form Solutions

3.1 Overview

In the following sections, linear least squares (LLS), weighted linear least squares (WLLS) and 2-step weighted linear least squares (2WLLS) mentioned in 1 and the Cramer-Rao lower bound (CRLB) are presented in 3.2, 3.3, 3.4 and 3.5 respectively, the last two of which will be employed in simulations in 4. Nonetheless, the first two methods are important bases for the formulation of the 2WLLS and therefore are described in this chapter as well. In each following section, formulation of the corresponding closed-form method for TOA-based localization is followed by that of closed-form method for TDOA-based localization.

3.2 Linear Least Squares

In order to find the target source location $\mathbf{u}^o$ from r_i with $i = 1, 2, \dots M$, in a closed-form, the measurement model needs to be linearized. As the first step of linearization, both sides of Equation 2.3 are squared and assuming that the distance measurement error is small, the second-order error terms are ignored, which gives

$$\begin{aligned} r_i^2 &\approx (x_i^o - x^o)^2 + (y_i^o - y^o)^2 + 2r_i^o n_i \\ &= x_i^{o2} + y_i^{o2} + x^{o2} + y^{o2} - 2(x_i^o x^o + y_i^o y^o) + 2r_i^o n_i \\ &= \mathbf{s}_i^o \mathbf{s}_i^{oT} + \mathbf{u}^o \mathbf{u}^{oT} - 2\mathbf{s}_i^o \mathbf{u}^{oT} + 2r_i^o n_i. \end{aligned} \tag{3.1}$$

As mentioned in 2.1.2 and 2.2.2, the true sensor node position is $\mathbf{s}_i^o = \mathbf{s}_i - \mathbf{n}_{si}$ where $\mathbf{n}_{si}$ is the sensor position error which is assumed to be zero-mean Gaussian with σ_{si}. Replacing the true sensor positions $\mathbf{s}_i^o$ by $\mathbf{s}_i - \mathbf{n}_{si}$ yields

$$r_i^2 = \mathbf{s}_i \mathbf{s}_i^T + \mathbf{u}^o \mathbf{u}^{oT} + 2(\mathbf{u}^o - \mathbf{s}_i)\mathbf{n}_{si}^T - 2\mathbf{s}_i \mathbf{u}^{oT} + 2r_i^o n_i \tag{3.2}$$

Denote an error $e_i = 2r_i^o n_i + 2(\mathbf{u}^o - \mathbf{s}_i)\mathbf{n}_{si}^T$ and a new variable $P_i = \mathbf{s}_i\mathbf{s}_i^T$, Equation 3.2 for all sensors can be written in a matrix form as

$$\mathbf{e} = \mathbf{h}_1 - \mathbf{G}_1\boldsymbol{\eta}_1, \tag{3.3}$$

where

$$\mathbf{h}_1 = \begin{bmatrix} r_1^2 - P_1 \\ \vdots \\ r_M^2 - P_M \end{bmatrix}, \mathbf{G}_1 = -2\begin{bmatrix} \mathbf{s}_1 & -\frac{1}{2} \\ \vdots & \vdots \\ \mathbf{s}_M & -\frac{1}{2} \end{bmatrix}, \eta_1^o = \begin{bmatrix} \mathbf{u}^{oT} \\ \mathbf{u}^o\mathbf{u}^{oT} \end{bmatrix} \tag{3.4}$$

Using Equation 3.3, the cost function for the LLS is given as

$$\begin{aligned} J_{LLS,TOA}(\hat{\boldsymbol{\eta}}_1) =& (\mathbf{h}_1 - \mathbf{G}_1\hat{\boldsymbol{\eta}}_1)^T(\mathbf{h}_1 - \mathbf{G}_1\hat{\boldsymbol{\eta}}_1) \\ =& \mathbf{h}_1^T\mathbf{h}_1 - 2\hat{\boldsymbol{\eta}}_1^T\mathbf{G}_1^T\mathbf{h}_1 + \hat{\boldsymbol{\eta}}_1^T\mathbf{G}_1^T\mathbf{G}_1\hat{\boldsymbol{\eta}}_1. \end{aligned} \tag{3.5}$$

The solution of the LLS is $\hat{\boldsymbol{\eta}}_1$ for which the cost function is at its global minimum. The global minimum can be found by taking the derivative of the cost function with respect to $\hat{\boldsymbol{\eta}}_1$ and setting it to zero as

$$\frac{\mathrm{d}J_{LLS,TOA}}{\mathrm{d}\hat{\boldsymbol{\eta}}_1} = -2\mathbf{G}_1^T\mathbf{h}_1 + 2\mathbf{G}_1^T\mathbf{G}_1\hat{\boldsymbol{\eta}}_1 = \mathbf{0}, \tag{3.6}$$

and solving for $\hat{\boldsymbol{\eta}}_1$ gives the LLS solution for the TOA-based localization as

$$\hat{\boldsymbol{\eta}}_1 = (\mathbf{G}_1^T\mathbf{G}_1)^{-1}\mathbf{G}_1^T\mathbf{h}_1. \tag{3.7}$$

As for the formulation of the LLS method for the TDOA-based localization, in the same manner as in Equation 3.1, squaring both sides of Equation 2.7 and ignoring the second order error terms yields

$$\begin{aligned} r_{i1}^2 \approx& (x_i^o - x^o)^2 + (y_i^o - y^o)^2 - (x_1^o - x^o)^2 - (y_1^o - y^o)^2 \\ & - 2r_{i1}\sqrt{(x_1^o - x^o)^2 + (y_1^o - y^o)^2} + 2n_{i1}\sqrt{(x_i^o - x^o)^2 + (y_i^o - y^o)^2} \\ =& x_i^{o2} + y_i^{o2} + x_1^{o2} + y_1^{o2} - 2(x_i^o x^o + y_i^o y^o - x_1^o x^o - y_1^o y^o) - 2r_{i1}^o r_1^o + 2r_i^o n_{i1} \\ =& \mathbf{s}_i^o\mathbf{s}_i^{oT} - \mathbf{s}_1^o\mathbf{s}_1^{oT} - 2(\mathbf{s}_i^o - \mathbf{s}_1^o)\mathbf{u}^{oT} - 2r_1^o r_{i1} + 2r_i^o n_{i1}. \end{aligned} \tag{3.8}$$

Similarly as in the TOA-based localization, the outdoor TDOA-based localization scenario where the UAVs are deployed as sensors of the measurements leads to the sensor position uncertainty due to the mobility of the UAVs and the inaccuracy of the GPS unit, as described in 2.2.2. Again, let the true position of the ith sensor be $\mathbf{s}_i^o = \mathbf{s}_i - \mathbf{n}_{si}$ where $\mathbf{n}_{si}$ is the error between the true position of ith sensor $\mathbf{s}_i^o$ and the measured position of ith sensor $\mathbf{s}_i$ while $P_i = \mathbf{s}_i\mathbf{s}_i^T$. Then, Equation 3.8 becomes

$$r_{i1}^2 \approx \mathbf{s}_i^o\mathbf{s}_i^{oT} - \mathbf{s}_1^o\mathbf{s}_1^{oT} - 2(\mathbf{s}_i^o - \mathbf{s}_1^o)\mathbf{u}^{oT} - 2r_1^o r_{i1} + 2r_i^o n_{i1} + 2(\mathbf{u^o} - \mathbf{s}_i)\mathbf{n}_{si}{}^T - 2(\mathbf{u}^o - \mathbf{s}_1)\mathbf{n}_{s1}^T, \tag{3.9}$$

where the second order error term is ignored. Knowing that the error in ith TDOA range measurement in Equation 3.9 can be expressed as

$$\begin{aligned} e_i =& 2r_i^o n_{i1} + 2(\mathbf{u^o} - \mathbf{s}_i){\mathbf{n}_{si}}^T - 2(\mathbf{u}^o - \mathbf{s}_1)\mathbf{n}_{s1}^T \\ =& r_{i1}^2 - \mathbf{s}_i^o \mathbf{s}_i^{oT} + \mathbf{s}_1^o \mathbf{s}_1^{oT} + 2(\mathbf{s}_i^o - \mathbf{s}_1^o)\mathbf{u}^{oT} + 2r_1^o r_{i1}, \end{aligned} \tag{3.10}$$

the matrix form linear equation for all TDOA measurements can be formulated as

$$\mathbf{e} = \mathbf{h}_1 - \mathbf{G}_1 \boldsymbol{\varphi}_1^o, \tag{3.11}$$

where

$$\mathbf{h}_1 = \begin{bmatrix} r_{21}^2 - R_2 + R_1 \\ r_{31}^2 - R_3 + R_1 \\ \vdots \\ r_{M1}^2 - R_M + R_1 \end{bmatrix}, \mathbf{G}_1 = -2 \begin{bmatrix} (\mathbf{s}_2 - \mathbf{s}_1)^T & r_{21} \\ (\mathbf{s}_3 - \mathbf{s}_1)^T & r_{31} \\ \vdots & \vdots \\ (\mathbf{s}_M - \mathbf{s}_1)^T & r_{M1} \end{bmatrix}, \boldsymbol{\varphi}_1^o = \begin{bmatrix} \mathbf{u}^{oT} \\ r_1^o \end{bmatrix} \tag{3.12}$$

Following the same derivations as in Equations 3.5, 3.6 and 3.7, the LLS solution for the TDOA-based localization is

$$\hat{\boldsymbol{\varphi}}_1 = (\mathbf{G}_1^T \mathbf{G}_1)^{-1} \mathbf{G}_1^T \mathbf{h}_1. \tag{3.13}$$

To avoid any confusions, it must be noted that although the same symbols $\mathbf{h}_1$ and $\mathbf{G}_1$ are used for the solutions of both TOA- and TDOA-based localizations in Equations 3.7 and 3.13, they are different from each other as defined in Equations 3.4 and 3.12, respectively.

3.3 Weighted Linear Least Squares

As mentioned in 3.2, the LLS method obtains the target location estimate by achieving the global minimum of the given cost function which is a square of the error vector $\mathbf{e}$. Knowing that the error $e_i = 2r_i^o n_i + 2(\mathbf{u}^o - \mathbf{s}_i)\mathbf{n}_{si}^T$, the error vector $\mathbf{e}$ for the TOA-based localization in Equation 3.3 can also be expressed by

$$\mathbf{e} = \mathbf{V}_1 \mathbf{n}_r + \mathbf{O}_1 \mathbf{n}_s \tag{3.14}$$

where

$$\mathbf{V}_1 = 2 \begin{bmatrix} r_1^o & \cdots & 0 \\ \vdots & \ddots & \vdots \\ 0 & \cdots & r_M^o \end{bmatrix}, \mathbf{O}_1 = \begin{bmatrix} (\mathbf{u}^o - \mathbf{s}_1) & \cdots & \mathbf{0}_{1\times 2} \\ \vdots & \ddots & \vdots \\ \mathbf{0}_{1\times 2} & \cdots & (\mathbf{u}^o - \mathbf{s}_M) \end{bmatrix} \tag{3.15}$$

, $\mathbf{n}_r = [n_1, \ldots, n_M]^T$ and $\mathbf{n}_s = [\mathbf{n}_{s1}^T, \ldots, \mathbf{n}_{sM}^T]^T$. Since each element in the noise vectors $\mathbf{n}_r$ and $\mathbf{n}_s$ is zero-mean Gaussian error, it is clear that the target location estimate obtained by the LLS method is accurate only when all errors in the noise vectors are independent and identically distributed. In practical situations however, this condition is rarely the case

if not impossible as the STD of each error varies depending on the distance between the corresponding sensor node and the target, or the mobility of the corresponding sensor node, which makes the LLS suboptimal. To improve the accuracy of the estimation, a weighting matrix can be utilized as

$$\hat{\boldsymbol{\eta}}_1 = (\mathbf{G}_1^T \mathbf{W}_1 \mathbf{G}_1)^{-1} \mathbf{G}_1^T \mathbf{W}_1 \mathbf{h}_1 \tag{3.16}$$

where the weighting matrix is an inverse of the covariance matrix of the error vector $\mathbf{e}$, given by

$$\mathbf{W}_1 = cov^{-1}[\mathbf{e}], \tag{3.17}$$

and the covariance is given by

$$cov[\mathbf{e}] = E[\mathbf{e}^T\mathbf{e}] + E[\mathbf{e}]^T E[\mathbf{e}] = 4diag[\sigma_1^2, \sigma_2^2, \ldots \sigma_M^2] + 4diag[\sigma_{s1}^2, \sigma_{s2}^2, \ldots \sigma_{sM}^2], \tag{3.18}$$

where E denotes a mean value and $diag$ denotes a diagonal matrix. Equation 3.16 is the WLLS estimator for the TOA-based localization. Now, since the weighting matrix is an inverse of the covariance matrix, the weighting matrix modifies the LLS solution in a way that the noisy measurements are suppressed according to the STDs and thereby, yielding the target location estimate with a higher accuracy than the LLS method.

As for the WLLS for the TDOA-based localization, the same formulation procedures can be used: knowing that the error of the range measurement on the ith is $e_i = 2r_i^o n_{i1} + 2(\mathbf{u^o} - \mathbf{s}_i)\mathbf{n}_{si}{}^T - 2(\mathbf{u}^o - \mathbf{s}_1)\mathbf{n}_{s1}^T$, the error vector $\mathbf{e}$ can be expressed as

$$\mathbf{e} = \mathbf{B}_1\mathbf{n}_r + \mathbf{D}_1\mathbf{n}_s, \tag{3.19}$$

where

$$\mathbf{B}_1 = 2\begin{bmatrix} r_2^o & 0 & \cdots & 0 \\ 0 & r_3^o & \cdots & 0 \\ \vdots & \vdots & \ddots & 0 \\ 0 & 0 & \cdots & r_M^o \end{bmatrix}, \mathbf{D} = 2\begin{bmatrix} -(\mathbf{u}^o - \mathbf{s}_1) & (\mathbf{u}^o - \mathbf{s}_2) & \mathbf{0}_{1\times 2} & \cdots & \mathbf{0}_{1\times 2} \\ -(\mathbf{u}^o - \mathbf{s}_1) & \mathbf{0}_{1\times 2} & (\mathbf{u}^o - \mathbf{s}_3) & \cdots & \mathbf{0}_{1\times 2} \\ \vdots & \vdots & \vdots & \ddots & \vdots \\ -(\mathbf{u}^o - \mathbf{s}_1)^T & \mathbf{0}_{1\times 2} & \mathbf{0}_{1\times 2} & \cdots & (\mathbf{u}^o - \mathbf{s}_M) \end{bmatrix} \tag{3.20}$$

, $\mathbf{n}_r = [n_{21}, \ldots, n_{M1}]^T$ and $\mathbf{n}_s = [\mathbf{n}_{s1}^T, \mathbf{n}_{s2}^T, \mathbf{n}_{s1}^T, \mathbf{n}_{s3}^T \ldots, \mathbf{n}_{s1}^T, \mathbf{n}_{sM}^T]^T$. Similarly as in the derivations of the weighting matrix for the TOA-based localization, the weighting matrix for the TDOA can be derived by taking the inverse of the covariance of $\mathbf{e}$, which can be simplified into

$$\mathbf{W}_1 = (\mathbf{B}_1\mathbf{Q}_r\mathbf{B}_1^T + \mathbf{D}_1\mathbf{Q}_s\mathbf{D}_1^T)^{-1}. \tag{3.21}$$

where $\mathbf{Q}_r$ and $\mathbf{Q}_s$ are the covariance matrices of the distance measurement error and the sensor position error respectively and are given by

$$\mathbf{Q}_r = \begin{bmatrix} \sigma_2 + \sigma_1 & \sigma_1 & \cdots & \sigma_1 \\ \sigma_1 & \sigma_3 + \sigma_1 & \cdots & \sigma_1 \\ \vdots & \vdots & \ddots & \vdots \\ \sigma_1 & \sigma_1 & \cdots & \sigma_M + \sigma_1 \end{bmatrix}, \ \mathbf{Q}_s = \begin{bmatrix} \sigma_{s1} & 0 & \cdots & 0 \\ 0 & \sigma_{s2} & \cdots & 0 \\ \vdots & \vdots & \ddots & \vdots \\ 0 & 0 & \cdots & \sigma_{sM} \end{bmatrix}. \tag{3.22}$$

From Equations 3.11, 3.12 and 3.21, the solution of the WLLS for the TDOA-based localization is

$$\boldsymbol{\varphi}_1 = (\mathbf{G}_1^T \mathbf{W}_1 \mathbf{G}_1)^{-1} \mathbf{G}_1^T \mathbf{W}_1 \mathbf{h}_1. \tag{3.23}$$

3.4 2-step Weighted Linear Least Square

Although $\mathbf{u}^o$ in the closed-form solution in Equation 3.16 is the estimate of the target position, the estimation is not accurate due to the fact that $\mathbf{u}^{oT}\mathbf{u}^o$ is assumed to be unrelated to $\mathbf{u}^o$ in order to solve the closed-form equation as a linear equation. To increase the accuracy of the estimate, refinement of the estimate through another formulation of the WLS method is needed. To refine $\boldsymbol{\eta}_1$, let $\boldsymbol{\Delta\eta_1}$ be the estimation error of $\boldsymbol{\eta_1}$, from which the relations between the estimate and the true position of the target can be formulated as

$$\boldsymbol{\eta}_1(1:2) \odot \boldsymbol{\eta}_1(1:2) \approx \mathbf{u}^o \odot \mathbf{u}^o + 2\mathbf{u}^o \odot \boldsymbol{\Delta\eta}_1(1:2) \tag{3.24}$$

and

$$\boldsymbol{\eta}_1(3) \approx \mathbf{u}^{oT}\mathbf{u}^o + \boldsymbol{\Delta\eta_1}(3) \tag{3.25}$$

The symbol $\odot$ represents element-by-element multiplication and $(\ )$ indicate the indices of the elements of the corresponding vector. Similar to the formulation of the linear equation in Equation 3.3, Equations 3.24 and 3.25 can be rearranged for the error in the initial estimation η_1 as

$$\mathbf{e}_2 = \mathbf{V}_2 \boldsymbol{\Delta\eta}_1 = \mathbf{h}_2 - \mathbf{G}_2 \boldsymbol{\eta}_2^o \tag{3.26}$$

where

$$\mathbf{V}_2 = diag[2x^o, 2y^o, 1], \mathbf{h}_2 = \boldsymbol{\eta}_1, \mathbf{G_2} = \begin{bmatrix} 1 & 0 \\ 0 & 1 \\ 1 & 1 \end{bmatrix}, \boldsymbol{\eta}_2^o = \mathbf{u}^o \odot \mathbf{u}^o = \begin{bmatrix} x^{o2} \\ y^{o2} \end{bmatrix} \tag{3.27}$$

To obtain the WLS solution of Equation 3.26 (or the 2WLLS solution for the TOA-based localization), the corresponding weighting matrix $\mathbf{W}_2$ is derived by calculating the inverse of the covariance of the error terms,

$$\mathbf{W}_2 = E[(\mathbf{V}_2 \boldsymbol{\Delta\eta}_1)(\mathbf{V}_2 \boldsymbol{\Delta\eta}_1)^T]^{-1} = \mathbf{V}_2^{-T} cov(\boldsymbol{\eta})_1^{-1} \mathbf{V}_2^{-1} \tag{3.28}$$

Using $\mathbf{W}_2$, the estimate of the $\hat{\boldsymbol{\eta}}_2^o$ which is the second stage solution of the 2WLLS is given by

$$\hat{\boldsymbol{\eta}}_2 = (\mathbf{G}_2^T \mathbf{W}_2 \mathbf{G}_2)^{-1} \mathbf{G}_2^T \mathbf{W}_2 \mathbf{h}_2. \tag{3.29}$$

As for the 2WLLS for the TDOA-based localization, in Equation 3.11, while the third element of variable $\boldsymbol{\varphi}_1^o$, which is r_1^o, is related to its first and second elements through the nonlinear equation in Equation 2.2, r_1^o is assumed to be unrelated to $\mathbf{u}^o$ in order to make

Equation 3.8 linear with respect to $\boldsymbol{\varphi}_1^o$ and obtain the WLS solution in the following. As a consequence of this assumption, the estimate $\boldsymbol{\varphi}_1^o$ becomes inaccurate. Therefore, the refinement of the estimate is necessary to increase the accuracy of the target location estimate. Again, let $\boldsymbol{\Delta\varphi}_1$ be the estimation error of $\boldsymbol{\varphi}_1^o$. The relation between the estimate of the first stage and the true target position can be expressed as

$$(\boldsymbol{\varphi_1}(\mathbf{1:2})-\mathbf{s}_1)\odot(\boldsymbol{\varphi_1}(\mathbf{1:2})-\mathbf{s}_1)=(\mathbf{u}^o-\mathbf{s}_1)\odot(\mathbf{u}^o-\mathbf{s}_1)+2(\mathbf{u}^o-\mathbf{s}_1)\odot\boldsymbol{\Delta\varphi_1}(1:2) \quad (3.30)$$

and

$$\boldsymbol{\varphi}_1(3)^2=(\mathbf{u}-\mathbf{s}_1)^T(\mathbf{u}-\mathbf{s}_1)+2(\mathbf{u}-\mathbf{s}_1)^T\boldsymbol{\Delta s}_1+2r_1^o\boldsymbol{\Delta\varphi}_1(3), \quad (3.31)$$

where the second order error terms are ignored. Using Equations 3.30 and 3.31, the linear vector form equation for the estimation error can be formulated as

$$\mathbf{e}_2=\mathbf{h}_2-\mathbf{G}_2\boldsymbol{\varphi}_2^o, \quad (3.32)$$

where

$$\mathbf{h}_2=\begin{bmatrix}(\boldsymbol{\varphi_1}(\mathbf{1:2})-\mathbf{s}_1)\odot(\boldsymbol{\varphi_1}(\mathbf{1:2})-\mathbf{s}_1)\\ \boldsymbol{\varphi}(3)^2\end{bmatrix},\mathbf{G}_2=\begin{bmatrix}1&0\\0&1\\1&1\end{bmatrix},\boldsymbol{\varphi}_2^o=\begin{bmatrix}(\mathbf{u}-\mathbf{s}_1)\odot(\mathbf{u}-\mathbf{s}_1)\end{bmatrix} \quad (3.33)$$

Alternatively, error vector $\mathbf{e}_2$ can be expressed by

$$\mathbf{e}_2=\mathbf{B}_2\boldsymbol{\Delta\varphi}_1+\mathbf{D}_2\boldsymbol{\Delta\beta}_1, \quad (3.34)$$

where

$$\mathbf{B}_2=2diag\begin{bmatrix}(\mathbf{u}-\mathbf{s}_1)^T & r_1^o\end{bmatrix},\mathbf{D}_2=\begin{bmatrix}\mathbf{0}_{2\times 2M}\\ 2(\mathbf{u}^o-\mathbf{s}_1)^T & \mathbf{0}_{1\times(2M-2)}\end{bmatrix} \quad (3.35)$$

As for the weighting matrix for the WLS solution of the linear equation in Equation 3.32, the weighting matrix is obtained by calculating the inverse of the covariance of the error vector $\mathbf{e}_2$, which is given by

$$\begin{aligned}\mathbf{W}_2&=E[\mathbf{e}_2\mathbf{e}_2^T]^{-1}\\&=(\mathbf{B}_2cov(\varphi)_1\mathbf{B}_2^T+\mathbf{D}_2\mathbf{Q}_\beta\mathbf{D}_2^T+\mathbf{B}_2(\mathbf{G}_1^T\mathbf{W}_1\mathbf{G}_1)^{-1}\mathbf{G}_1^T\mathbf{W}_1\mathbf{D}_1\mathbf{Q}_\beta\mathbf{D}_2^T\\&\quad+\mathbf{D}_2\mathbf{Q}_\beta\mathbf{D}_1^T\mathbf{W}_1\mathbf{G}_1(\mathbf{G}_1^T\mathbf{W}_1\mathbf{G}_1)^{-1}\mathbf{B}_2^T)^{-1}.\end{aligned} \quad (3.36)$$

Finally, the 2WLS solution of Equation 3.32 is

$$\boldsymbol{\varphi}_2=(\mathbf{G}_2^T\mathbf{W}_2\mathbf{G}_2)^{-1}\mathbf{G}_2^T\mathbf{W}_2\mathbf{h}_2. \quad (3.37)$$

3.5 Cramer-Rao Lower Bound

CRLB gives a lower bound on variance attainable by any unbiased location estimators for the same data set [6]. Thus, the CRLB can be used as a performance reference to the 2WLLS estimator. The CRLB for TOA-based localization is given by [7]

$$CRLB(\mathbf{u}^o) = [\mathbf{I}_{\text{TOA}}^{-1}(\mathbf{u}^o)]_{1,1} + [\mathbf{I}_{\text{TOA}}^{-1}\mathbf{u}^o]_{2,2} \tag{3.38}$$

where $\mathbf{I}_{\text{TOA}}(\mathbf{u}^o)$ denotes the Fisher information matrix (FIM). The FIM for the TOA-based localization is calculated as

$$\mathbf{I}_{\text{TOA}}(\mathbf{u}^o) = \left[\frac{\partial \mathbf{f}_{\text{TOA}}(\mathbf{u}^o)}{\partial \mathbf{u}^o}\right]^T \mathbf{C}_{\text{TOA}}^{-1} \left[\frac{\partial \mathbf{f}_{\text{TOA}}(\mathbf{u}^o)}{\partial \mathbf{u}^o}\right] \tag{3.39}$$

where $\mathbf{C}_{\text{TOA}}$ is a covariance matrix for the distance measurement error $\mathbf{n}_i$ and $\mathbf{f}_{\text{TOA}}(\mathbf{u}^o)$ is a vector of TOA range measurements, given by

$$\mathbf{C}_{\text{TOA}} = \begin{bmatrix} \sigma_1 & 0 & \cdots & 0 \\ 0 & \sigma_2 & \cdots & 0 \\ \vdots & \vdots & \ddots & \vdots \\ 0 & 0 & \cdots & \sigma_i \end{bmatrix}, \ \mathbf{f}_{\text{TOA}} = \begin{bmatrix} \sqrt{(x^o - x_1^o)^2 + (y^o - y_1^o)^2} \\ \vdots \\ \sqrt{(x^o - x_i^o)^2 + (y^o - y_i^o)^2} \end{bmatrix} \tag{3.40}$$

The simplified FIM is expressed as

$$\mathbf{I}_{\text{TOA}}(\mathbf{u}^o) = \begin{bmatrix} \sum_{i=1}^{M} \frac{(x^o - x_i)^2}{\sigma_i r_i^{o2}} & \sum_{i=1}^{M} \frac{(x^o - x_i)(x^o - x_i)}{\sigma_i r_i^{o2}} \\ \sum_{i=1}^{M} \frac{(x^o - x_i)(x^o - x_i)}{\sigma_i r_i^{o2}} & \sum_{i=1}^{M} \frac{(y^o - y_i)^2}{\sigma_i r_i^{o2}} \end{bmatrix}. \tag{3.41}$$

Similarly, the CRLB for the TDOA-based localization is given by [8]

$$CRLB(\mathbf{u}^o) = [\mathbf{I}_{\text{TDOA}}^{-1}(\mathbf{u}^o)]_{1,1} + [\mathbf{I}_{\text{TDOA}}^{-1}\mathbf{u}^o]_{2,2} \tag{3.42}$$

where

$$\mathbf{I}_{\text{TDOA}}(\mathbf{u}^o) = \left[\frac{\partial \mathbf{f}_{\text{TDOA}}(\mathbf{u}^o)}{\partial \mathbf{u}^o}\right]^T \mathbf{C}_{\text{TDOA}}^{-1} \left[\frac{\partial \mathbf{f}_{\text{TDOA}}(\mathbf{u}^o)}{\partial \mathbf{u}^o}\right]. \tag{3.43}$$

and

$$\mathbf{C}_{\text{TDOA}} = \begin{bmatrix} \sigma_2 + \sigma_1 & \sigma_1 & \cdots & \sigma_1 \\ \sigma_1 & \sigma_3 + \sigma_1 & \cdots & \sigma_1 \\ \vdots & \vdots & \ddots & \vdots \\ \sigma_1 & \sigma_1 & & \sigma_i + \sigma_1 \end{bmatrix},$$

$$\mathbf{f}_{\text{TDOA}} = \begin{bmatrix} \sqrt{(x^o - x_2^o)^2 + (y^o - y_2^o)^2} - \sqrt{(x^o - x_1^o)^2 + (y^o)^2 - y_1^o} \\ \vdots \\ \sqrt{(x^o - x_i^o)^2 + (y^o - y_i^o)^2} - \sqrt{(x^o - x_1^o)^2 + (y^o)^2 - y_1^o} \end{bmatrix} \tag{3.44}$$

In this chapter, two closed-form solutions are presented for estimating target location from a set of TOA/TDOA measurements are presented, which incorporate the distance measurement error and the sensor position error. In the following, the performance of the closed-form solutions is investigated in the presence of the distance measurement error and the sensor position error.

Chapter 4

Simulation results

4.1 Overview

The localization scenario considered here incorporates two measurement error sources, i.e., distance measurement error and sensor position error due to the mobility of the sensor node, e.g., positioned on an UAV. The corresponding research questions are: 1) What is the localization accuracy of TOA- and TDOA-based localization in the presence of the anchor node position error and the distance measurement error?, 2) What is the effect of a geometrical configuration of sensor nodes on location estimation performance? and 3) Which one of the localization techniques is more suitable in presence of sensor position uncertainty? To answer the research questions, this chapter is organized as follows. In 4.2, the general simulation set-up for both TOA and TDOA is described, which includes the different geometrical deployments of the sensors. In 4.3, first the measurement error and the sensor position error are separately introduced to the TOA localization with square node deployment and to investigate the effect of each error independently. Then, square shape and triangular deployments are compared to examine the effect of the geometry of the sensor deployment. In 4.4, the same simulation sets as in 4.3 but for the TDOA are investigated. Finally in 4.5, the TOA and TDOA localization results for both geometrical configurations are compared given a certain range of sensor position error and a fixed value standard deviation of the distance measurement error.

4.2 Simulation Set-up

Simulations in the following sections run with $M = 4$ sensors. For configurations of sensor deployment, two deployments are considered: a square deployment and a triangular deployment. Sensor positions of the square and the triangular deployments are listed in Tables 4.1 and 4.2, respectively. As TDOA-based localization requires a reference sensor node, a sensor with sensor number $i = 1$ is used as a reference sensor. Regarding the

the distance measurement error and the sensor position error, zero-mean Gaussian errors are considered. As for evaluation of performance of the TOA- and the TDOA-based localization, a root-mean-square position error (RMSPE) is used as an indicator of localization performance, which is defined as RMSPE $= \sqrt{\frac{1}{L}\sum_{l=1}^{L}||\hat{\mathbf{u}}_l - \mathbf{u}^o||}$ where $\hat{\mathbf{u}}_l$ denotes an estimated location of the target at ensemble l and L is the number of ensemble runs. For all simulations, the number of ensemble runs is 10^5.

Table 4.1: Sensor positions for square deployment

Sensor number i	x_i(m)	y_i(m)
1	0	0
2	0	1000
3	1000	1000
4	1000	0

Table 4.2: Sensor positions for triangular deployment

Sensor number i	x_i(m)	y_i(m)
1	500	250
2	1000	0
3	500	866
4	0	0

4.3 TOA

First, the 2WLLS for the TOA localization with the square shape sensor deployment with sensor positions compiled in Table 4.1 and the target source located at $u^o = [700,\ 700]$ was evaluated, in which the distance measurement error and the sensor position error are applied by varying σ_1 and σ_p separately. It must be noted that when varying σ_1, the other standard deviations σ_2,σ_3 and σ_4 are varied relative to σ_1 and the ratio of d_2, d_3 and d_4 to d_1, i.e., $\boldsymbol{\sigma}_n = \sigma_1[1,\ \frac{d_2}{d_1},\ \frac{d_3}{d_1},\ \frac{d_4}{d_1}] = \sigma_1[1,\ 0.7693,\ 0.4286,\ 0.7693]$, which preserves the geometric feature that determines the value of each standard deviation. The results are depicted in Figure 4.1. In both results, the RMSPE linearly increases as the standard deviation of the measurement error σ_1 and the standard deviation of the sensor position error σ_p increase. When comparing Figure 4.1 (a) and (b) however, it is evident that the sensor position uncertainty error leads to a slightly higher rate of increase of the RMSPE than the measurement noise. Since σ_1 of 10m results in RMSPE of 6.985m in (a) while the RMSPE at σ_p of 10m in (b) is 10.1m, the sensor position uncertainty error gives approximately 1.446 times (or 3.203dB) higher RMSPE than the measurement noise.

To examine the effect of the sensor position uncertainty error on the TOA localization in presence of distance measurement error, the parametric sweeps of σ_p with $\sigma_1 = 4.742$m and $\sigma_1 = 10$m were performed and the results are shown in Figure 4.2. Again, the standard deviations of the measurement noise for the rest of the sensors are calculated relative to σ_1 and the ratio of their target-sensor distance to d_1, i.e., $\boldsymbol{\sigma}_n = [4.742,\ 3.648,\ 2.032,\ 3.648]$m for $\sigma_1 = 4.742$m and $\boldsymbol{\sigma}_n = [10,\ 7.693,\ 4.286,\ 7.693]$m for $\sigma_1 = 10$m. In Figure 4.2, RMSPEs of the 2WLLS at $\sigma_p = 10$m are 10.96m and 12.73m for $\sigma_1 = 4.742$m and $\sigma_1 = 10$m,

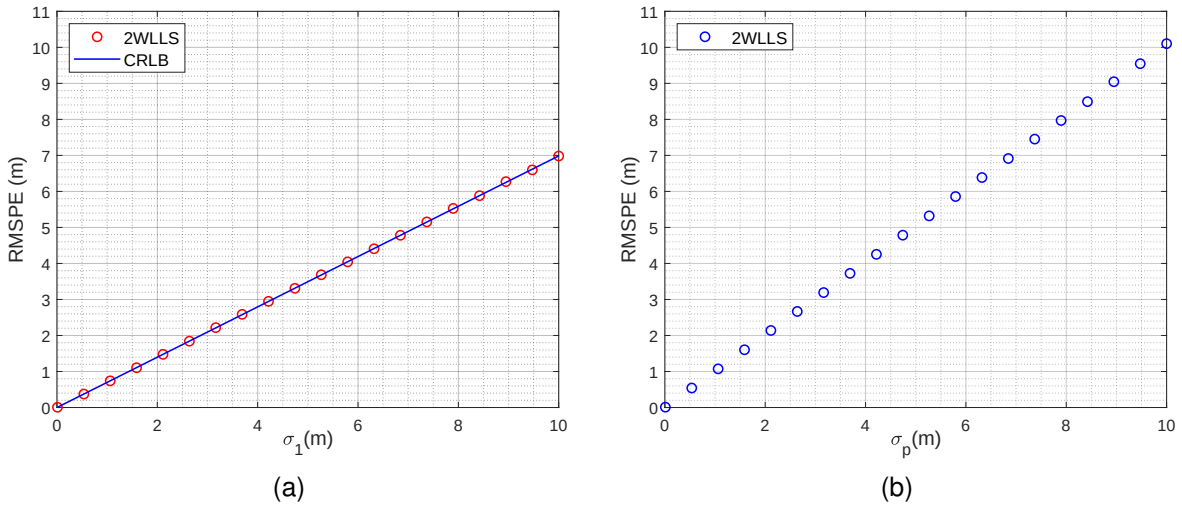

Figure 4.1: TOA localization performance for a square deployment: (a) with TOA distance measurement error and without sensor position error, and (b) with sensor position error and without TOA distance measurement error

respectively. When comparing these RMSPEs with the ones in Figure 4.1 (a) and (b), that are, RMSPEs of 3.313m and 6.985m at $\sigma_1 = 4.742$m and $\sigma_1 = 10$m respectively and RMSPE of 10m at $\sigma_p = 10$m, it can be noticed that the sums of the corresponding two RMSPEs at the given points, that are, $3.313 + 10 = 13.31$m and $6.985 + 10 = 16.98$m are not equal to the specified RMSPEs in Figure 4.2. This indicates that the sensor position uncertainty error and the measurement noise do not independently contribute to the RMSPE, but rather result in a smaller RMSPE than the sum of the two independently obtained RMSPEs.

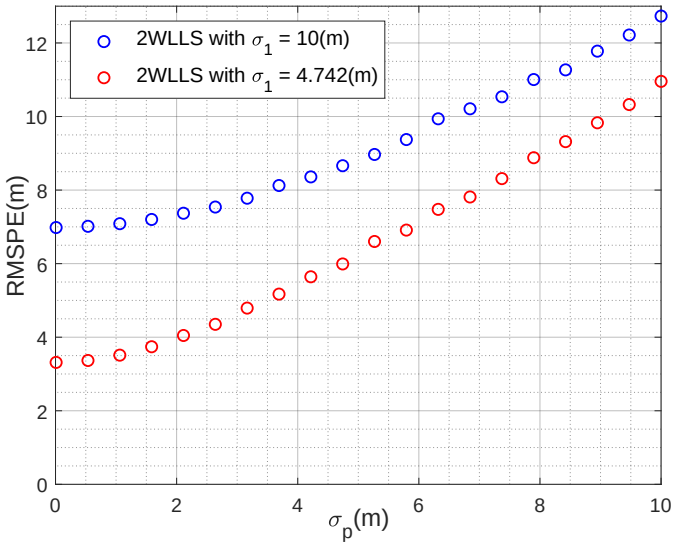

Figure 4.2: TOA localization performance for a square deployment as a function of sensor position error STD σ_p with σ_1 fixed at 4.742m and 10m

As one of the research questions in this paper is to investigate the effect of the sensor deployments, the comparisons between the square and the triangular deployments of the sensors are made in Figure 4.3, where the distance measurement noise and the sensor position error are introduced and swept separately. It can be observed that the RMSPE of the triangular shape deployment at $\sigma_1 = 10$m is 10.46m and RMSPE of the square deployment at $\sigma_1 = 10$m is 6.982m, meaning that the RMSPE of the square deployment is circa 1.492 times (or 3.478dB) smaller than that of the triangular deployment. In Figure 4.3, RMSPE of the triangular deployment at $\sigma_p = 10$m is 10.46m whilst RMSPE of the square deployment is 10.10m which is 1.032 times (or 0.2709dB) smaller than the RMSPE of the triangular deployment. Based on the difference of the RMSPEs between the two deployments, the triangular deployment is remarkably more prone to the estimation error caused by the measurement noise than the square deployment whereas the difference of the estimation errors between the two caused by the sensor position uncertainty error is minimal.

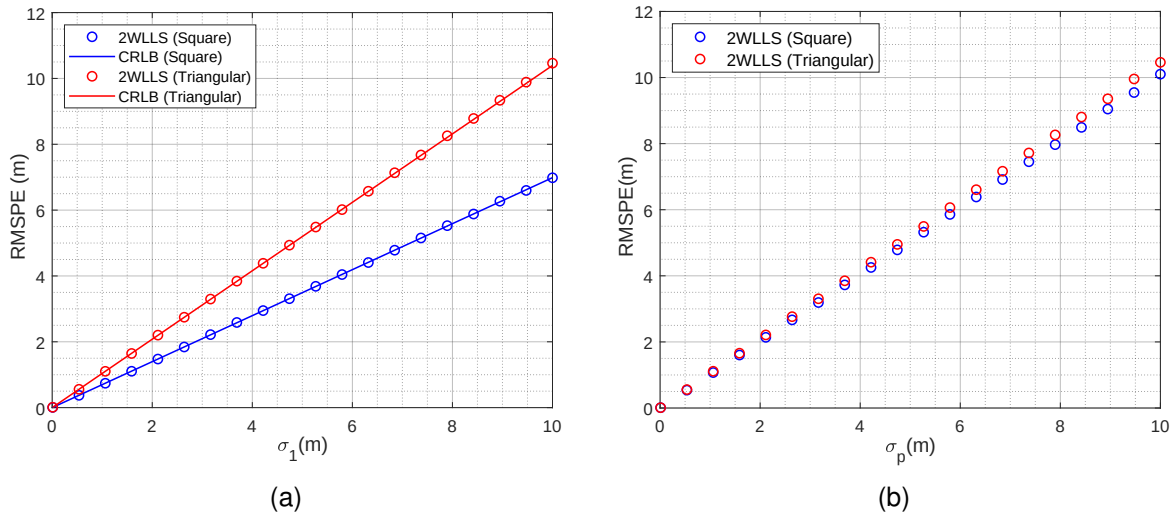

Figure 4.3: TOA localization performance for square and triangular deployments (a) without mobility and (b) with mobility

To further investigate the effect of the sensor deployment, the distance measurement error and the sensor position error are combined in the same manner as in Figure 4.2 and the two deployments are compared. The results are depicted in Figure 4.4. It can be seen that the rates of increase of the RMSPE in 2WLLS for both deployments are almost identical whilst the overall RMSPE of the triangular deployment is higher than that of the square-shape deployment, which correspond to the observations made in Figure 4.3. Furthermore, in line with the previous finding that the RMSPE of the square deployment in presence of both the measurement error and the sensor position uncertainty error in Figure 4.2 is smaller than the sum of the two RMSPEs obtained separately in Figure 4.1, the triangular deployment in presence of the measurement noise combined with the

sensor position uncertainty error in Figure 4.4 results in a smaller RMSPE than the sum of the two separate RMSPEs in Figure 4.3.

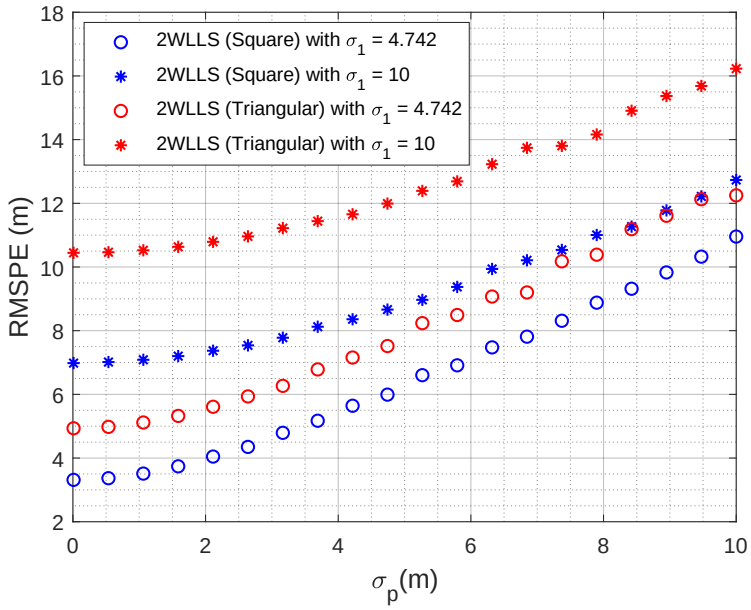

Figure 4.4: TOA localization performance for a square- and a triangular-shape deployments with σ_1 fixed at 4.742m and $10m$ for various σ_p

4.4 TDOA

This subsection presents results for the 2WLLS method and the TDOA localization. The 2WLLS for the TDOA localization with the square deployment (see Table 4.1) and the target source located at $u^o = [700,\ 700]$ is evaluated. Again, it must be noted that when varying σ_1, the other standard deviations σ_2,σ_3 and σ_4 are varied relative to σ_1 and the ratio of d_2, d_3 and d_4 to d_1, i.e., $\boldsymbol{\sigma}_n = \sigma_1[1,\ \frac{d_2}{d_1},\ \frac{d_3}{d_1},\ \frac{d_4}{d_1}] = \sigma_1[1,\ 0.7693,\ 0.4286,\ 0.7693]$. The resulting RMSPEs are depicted in Figure 4.5. In Figure 4.5 (a), it can be seen that the RMSPE of the 2WLLS starts to quickly diverge from the CRLB approximately after $\sigma_1 = 4$m and increases gradually non-linearly . In Figure 4.5 (b), the RMSPE of the 2WLLS increases linearly until circa $\sigma_p = 5$m and also starts to increase non-linearly afterwards. A possible reason for this difference is because that as the TDOA range measurement is a hyperbolic equation, the measurement errors quadratically impact the intersection of the hyperbole or the global minimum point, leading to a greater estimate error for the TDOA-based localization than that for the TOA-based localization. The maximum RMSPEs in Figure 4.5 (a) and (b) are 9.209m at $\sigma_1 = 10$m and 12.52m at $\sigma_p = 10$m, showing that the estimation error caused by the measurement noise is circa 1.360 times (or 2.668dB) smaller than that caused by the sensor position uncertainty error. Therefore, whilst both

RMSPEs exibit the similar trend pattern, the sensor position uncertainty error has more impact on the accuracy of the location estimate than the measurement error.

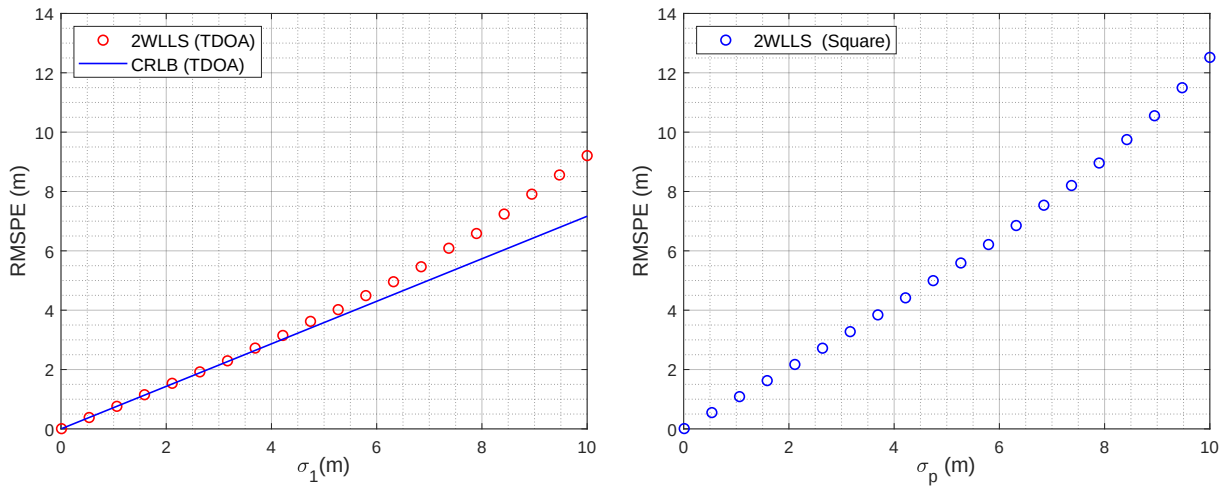

Figure 4.5: TDOA localization performance for a square-shape deployment (a) with TDOA distance measurement error and without sensor position error, and (b) with sensor position error and without TDOA distance measurement error

In the same manner as in Figure 4.2, the parametric sweeps of σ_p with σ_1 fixed at 4.742m and 10m are performed on the TDOA localization for the square deployment. The results are depicted in Figure 4.6. The RMSPEs of the 2WLLS for both σ_1 increase non-linearly for the entire range, which does not correspond to the observation made in Figure 4.5. The values of the RMSPE at $\sigma_p = 0$m and $\sigma_p = 10$m in Figure 4.6 are 3.591m and 15.61m for $\sigma_1 = 4.742$m and 9.143m and 22.75m for $\sigma_1 = 10$m. When comparing these values with the RMSPEs in Figure 4.5 for the given points of the standard deviations, i.e., RMSPE of 3.623m and 9.209m at $\sigma_1 = 4.742$m and 10m respectively, and RMSPE of 12.52m at $\sigma_p = 10$m, it can be noticed that the sum of the RMSPEs from 4.5, i.e., $3.623 + 12.52 = 16.14$m and $9.209 + 12.52 = 21.73$m, are almost equivalent to the RMSPEs from Figure 4.6. Therefore, it can be concluded that for the TDOA localization with the 2WLLS, the distance measurement error and the sensor position error independently affect the accuracy of the location estimation in an almost independent way.

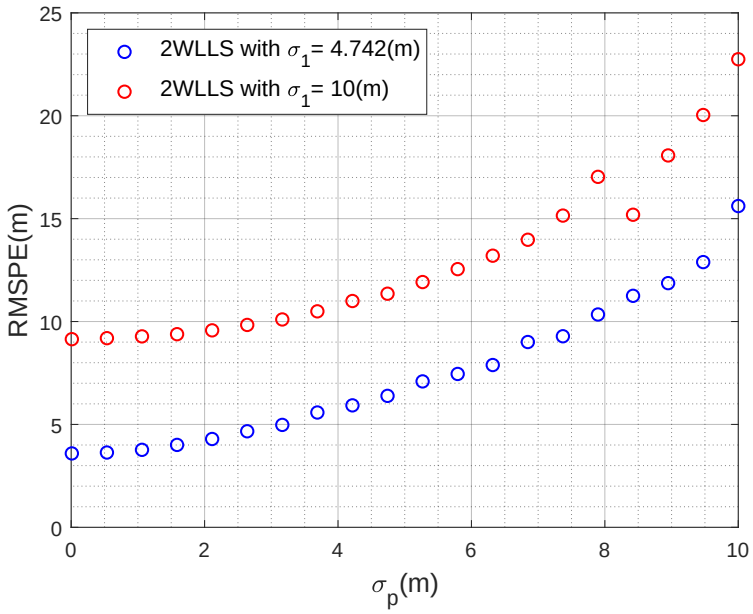

Figure 4.6: TDOA localization performance for a square-shape deployments with σ_1 fixed at 4.742m and 10m for various σ_p

To investigate the effect of the distance measurement error and the sensor position error on the performance of the localization estimate for different sensor deployments, the TDOA localization with the triangular deployment is also implemented. The results of the triangular deployment along with the result shown in Figure 4.5 are depicted in Figure 4.7. As can be seen in Figure 4.7, the TDOA localization with the triangular deployment is more prone to the location estimate error in both presences of the measurement noise and the sensor position uncertainty error than the TDOA localization with the square deployment. Quantitatively, the RMSPE of the square deployment is circa 3 times (or 9.5dB) less than that of the triangular deployment in presence of the measurement error and circa 1.3 times (or 2.3dB) less than that of the triangular deployment in presence of the sensor position uncertainty error.

In order to further examine the difference in RMSPE between the two deployments in case of both distance measurement error and sensor position error exist together, the RMSPEs of both deployments for various σ_p and fixed values of σ_1 are implemented and the results are depicted in Figure 4.8. In line with the observations made in Figure 4.7, the triangular deployment has higher RMSPE throughout the entire considered range of σ_p for $\sigma_1 = 4.742$m and $\sigma_1 = 10$m. However, it can be seen that the RMSPE of the square deployment has higher rate of increase with respect to σ_p. From this, it could be concluded that while the triangular deployment is more sensitive to the distance measurement error than the square deployment, the square deployment is more sensitive to the sensor position error than the triangular deployment.

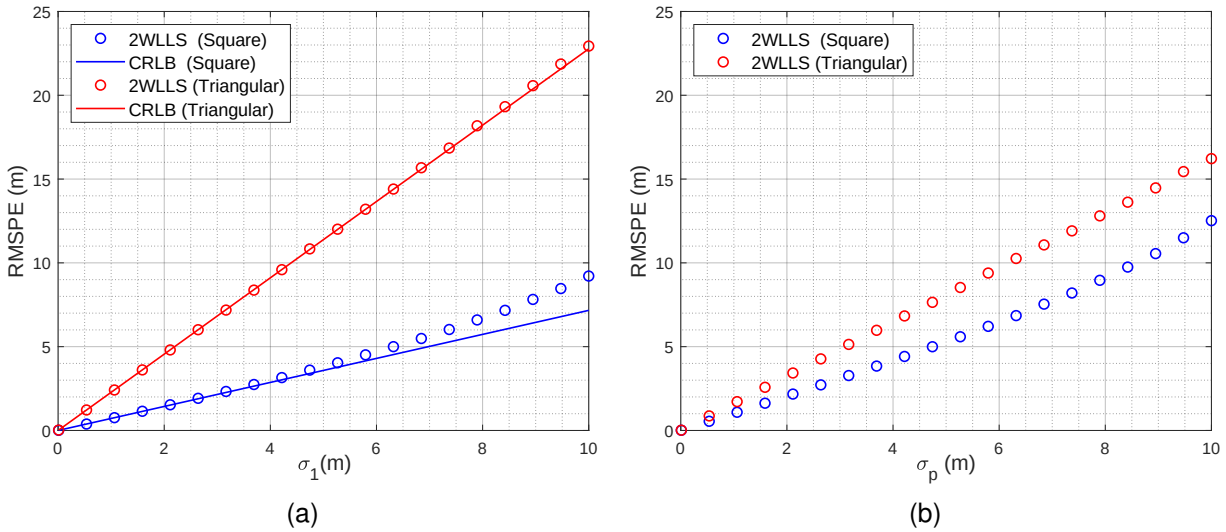

Figure 4.7: TDOA localization performance for square- and triangular-shape deployments (a) without mobility and (b) with mobility

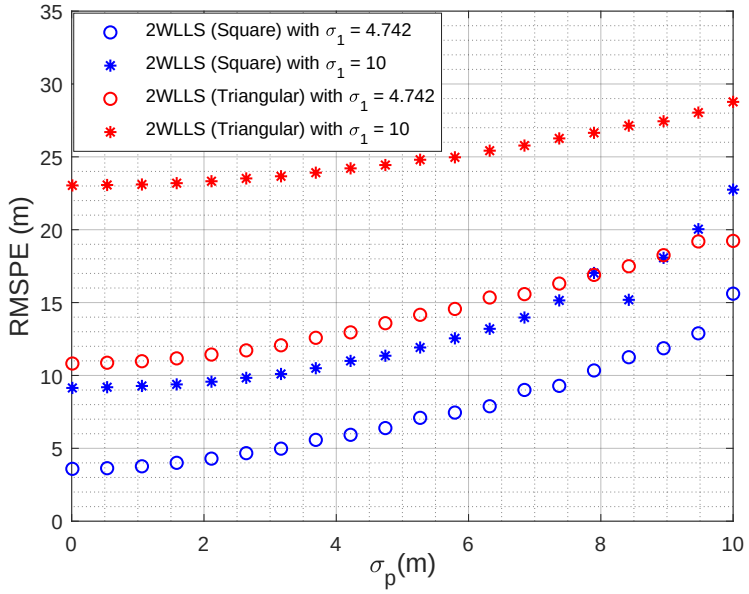

Figure 4.8: TDOA localization performance for square- and triangular-shape deployments as a function of σ_p with σ_1 fixed at 4.742m and 10m

4.5 Comparison between TOA and TDOA

Finally, here we compare the TOA and TDOA localization performance in the presence of both distance measurement noise and sensor position error. To do that, Figure 4.9 shows the results of the TOA and TDOA with the square and the triangular deployments for the distance measurement noise STD σ_1 fixed at 4.742m and the various sensor position

error STD σ_p. The RMSPEs of the 2WLLS for the TOA is circa 0.31dB lower than that for the TDOA in the range from $\sigma_p = 0$ to approximately $\sigma_p = 6.3$, after which the rate of increase of the RMSPE for the TDOA becomes high, the maximum difference being 1.5dB at $\sigma_p = 10$. Interestingly, although the TDOA has one independent measurement less than the TOA due to the unsynchronized target source and the sensors, the performance of the TDOA is not significantly worse than that of the TOA until σ_p reaches 6.3m. The comparison for the triangular deployment (see Figure 4.9 (b)) in contrast, shows that the TDOA has 10.82m at $\sigma_p = 0$m, 13.58m at $\sigma_p = 4.742$m and 19.23m at $\sigma_p = 10$m whilst the TOA has 4.934m, 7.517m and 12.25m, which is equivalent to the difference of 3.410dB, 2.578dB and 1.959dB respectively. From this, it is clear that although the difference in RMSPE between the two localization methods with the triangular deployment gradually becomes smaller for large $_p$, the difference is still significantly large. The TDOA with the triangular deployment is more sensitive to the measurement error than the TOA with the triangular deployment as the former has 3.410dB for $\sigma_p = 0$ and $\sigma_1 = 4.742$.

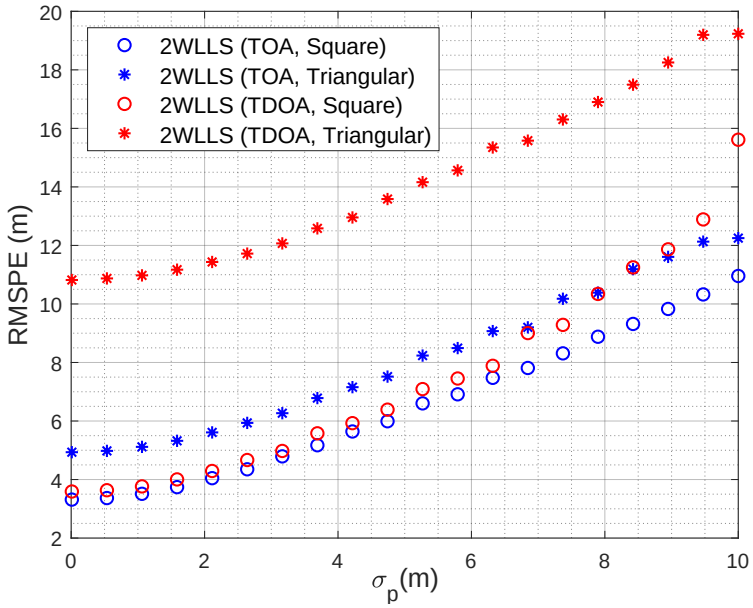

Figure 4.9: TOA and TDOA localizations with fixed measurement error variance $\sigma_1 = 4.742$m and various position uncertainty variance σ_p for square- and triangular- shape deployments

Although the comparison here is somewhat limited since the simulation is done for specific position of the target source, it does provide some insight of the effect of the sensor position error and the geometry of the sensor deployments. As touched upon before, it can be seen in Figure 4.9, that despite the fact that the TOA has an extra range measurement than the TDOA thanks to the target-sensor synchronization, the difference in accuracy between the TOA and the TDOA with the square deployment is rather minimal until the standard deviation reaches $\sigma_p = 6.3$m. It is particularly important to remark

that the typical standard deviation of GPS equipment is around 0.75m [9]. Furthermore, the target-sensor synchronization of the TOA is more technologically complex than the TDOA that is asynchronous. Keeping these in mind, when the quality of the GPS localization for the mobile sensors is not large, the TDOA with the square deployment could be considered optimal for the outdoor localization scenario using UAVs. As for the effect of the triangular sensor deployment on the localization performance, the comparisons in Figures 4.3 and 4.7 show that the triangular deployment for both TOA and TDOA results in the increase of the sensitivity to both measurement noise and sensor position error.

Chapter 5

Conclusion and Recommendations

Accuracies of TOA- and TDOA-localizations with mobile sensor nodes can be influenced by the mobility of sensor nodes as well as distance measurement error that is inherent in radio localization. In this work, the new 2WLLS methods proposed in [3] and [4] was performed with the square and the triangular sensor deployments. First, the localizaiton performance was evaluated when varying the variance of the Gaussian distributions of the distance measurement error and the sensor position error individually. Then, the two types of errors were combined together and the localization performance was evaluated for both TOA and TDOA. Finally, two different sensor deployment configurations have been evaluated and compared against each other.

Presented results indicate that although both TOA- and TDOA-based localization are more prone to an estimate error caused by the sensor position error, the two localizations showed different patterns of the performance curve: the root-mean-square position error (RMSPE) of the TOA-based locaization increase linearly with respect to the distance measurement error and the sensor position error whereas the RMSPE of the TDOA-based localization showed nonlinear relations to both measurement errors, which is possibly due to the characteristics of the hyperbolic equation. When the two measurement errors are combined, TOA- and TDOA-based localizations with the square sensor deployment showed a similar trend for a small STD of the sensor position error but the former had a RMSPE. For a large STD of the sensor position error, the TOA-based localization outperformed TDOA-based one. However, as discussed in 4.5, the typical value of the standard deviation for the GPS unit is around 0.75m and the performance difference between the two localizations for this value is 0.31dB. It is worth noting here that TOA-based localization is more technologically complex due to the need of the target-sensor synchronization. Therefore, regarding with the suitability of localization, it could be concluded the TDOA-based localization with the square deployment might be preferable, if one expects low to moderate sensor node position error.

As for the effect of the sensor configurations, the triangular configurations for both TOA- and TDOA-based localizations resulted in the increase of the sensitivity to both

measurement noise and the sensor position uncertainty error. Furthermore, it was observed that in the triangular configuration, the performance of the TDOA-based localization became significantly lower compared to the TOA-based localization. From this, it can be concluded that the triangular configuration is less suitable than the square configuration.

In this work, the 2WLLS method was implemented with the precise statistical knowledge of the STDs of the two types of errors involved. In practice however, the precision of the statistical knowledge may be limited. Therefore, an investigation of the sensitivity of the 2WLLS to an error in STD is a subject of further study. Furthermore, further investigation for the performance of the sensor deployments is recommended. The reason is that the comparisons between the triangular sensor configuration and the square sensor configuration are somewhat limited as the target location was fixed to $\mathbf{u}^o = [700, 700]$(m), while there might exist a location where the triangular sensor configuration could perform better.

Bibliography

[1] R. Zekavat and R. M. Buehrer, “Wireless positioning systems: Operation, application, and comparison,” 2019.

[2] H. So, “Source localization: Algorithms and analysis,” in *Handbook of Position Location: Theory, Practice, and Advances*. John Wiley & Sons, Inc., 2018, pp. 59–106.

[3] Z. Ma and K. Ho, “Toa localization in the presence of random sensor position errors,” in *2011 IEEE International Conference on Acoustics, Speech and Signal Processing (ICASSP)*. IEEE, 2011, pp. 2468–2471.

[4] K. Ho, X. Lu, and L.-o. Kovavisaruch, “Source localization using tdoa and fdoa measurements in the presence of receiver location errors: Analysis and solution,” *IEEE Transactions on Signal Processing*, vol. 55, no. 2, pp. 684–696, 2007.

[5] Y. T. Chan and K. Ho, “A simple and efficient estimator for hyperbolic location,” *IEEE Transactions on signal processing*, vol. 42, no. 8, pp. 1905–1915, 1994.

[6] E. G. Larsson, “Cramer-rao bound analysis of distributed positioning in sensor networks,” *IEEE Signal processing letters*, vol. 11, no. 3, pp. 334–337, 2004.

[7] F. Yin, C. Fritsche, F. Gustafsson, and A. M. Zoubir, “Toa-based robust wireless geolocation and cramér-rao lower bound analysis in harsh los/nlos environments,” *IEEE transactions on signal processing*, vol. 61, no. 9, pp. 2243–2255, 2013.

[8] R. Kaune, J. Hörst, and W. Koch, “Accuracy analysis for tdoa localization in sensor networks,” in *14th international conference on information fusion*. IEEE, 2011, pp. 1–8.

[9] J. R. Clynch, Feb 2001. [Online]. Available: https://www.oc.nps.edu/oc2902w/gps/gpsacc.html